IL NUOVO CIMENTO **42 C** (2019) 221
DOI 10.1393/ncc/i2019-19221-8

COMMUNICATIONS: SIF Congress 2018

The energy calibration procedure of the Muon $g-2$ experiment at Fermilab

M. SORBARA(*) on behalf of the MUON $g-2$ COLLABORATION

Università degli Studi di Roma Tor Vergata - Rome, Italy

received 8 April 2019

Summary. — The muon anomaly, a_μ, is a low energy observable that can be both measured and computed with high precision, therefore it provides an important test of the Standard Model (SM) and it is a sensitive probe for new physics. The Muon $g-2$ experiment at Fermilab aims to measure a_μ with a precision of 0.14 ppm, four times better than the previous experiment at BNL. In this paper I will introduce the calorimeter system and the energy calibration procedure using lost muons.

1. – Introduction

Muons are fundamental fermions with spin $s = \frac{1}{2}$ and mass $m_\mu = 105.658\,\text{MeV}$ [1]. The magnetic moment of a particle is expressed by the formula

$$\overrightarrow{\mu} = g_s \frac{e}{2m} \overrightarrow{s}, \tag{1}$$

where g_s is the giromagnetic factor, which is observed to be ~ 2 for fundamental particles.

Dirac's theory predicts the value $g_s = 2$ at the tree level, however higher order corrections can give a contribution to this value. So the muon anomaly can be written as

$$\frac{g-2}{2} = a_\mu = a_\mu^{QED} + a_\mu^{Weak} + a_\mu^{HVP} + a_\mu^{HLbL}, \tag{2}$$

with contributions from QED, weak interaction and QCD (that can be splitted in terms from Hadron Vacuum Polarization and Light by Light interaction). These contributions are represented by the diagrams shown in fig. 1.

(*) E-mail: matteo.sorbara@roma2.infn.it

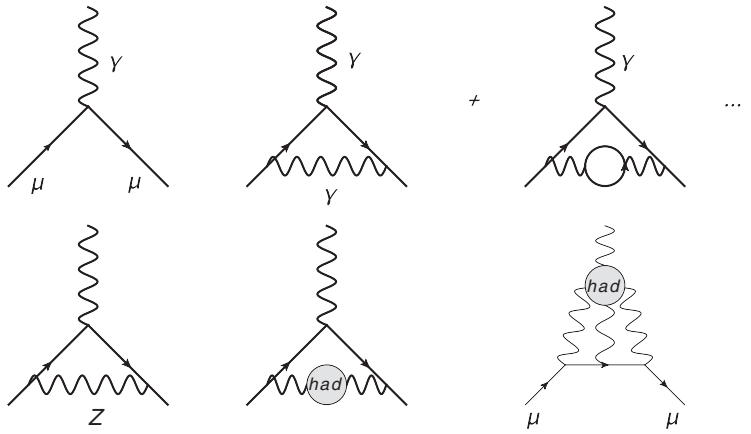

Fig. 1. – Feynman diagrams for the contributions to the $g-2$ value as presented in eq. (2). In the upper part the QED contribution, in the bottom part from left to right the Z_0, HVP and HLbL contributions.

From the experimental point of view, the world average of a_μ^{exp} is dominated by the measure at Brookheaven National Laboratory (BNL) in 2001. The measured value is [2]

$$a_\mu^{exp} = 11\ 695\ 208.9(6.3) \cdot 10^{-10} \quad [0.54\,\text{ppm}]. \tag{3}$$

The difference with the most recent Standard Model prediction [3] is

$$a_\mu^{exp} - a_\mu^{SM} = (27.06 \pm 7.26) \cdot 10^{-10}. \tag{4}$$

This difference corresponds to a 3.7σ discrepancy from the Standard Model prediction. This discrepancy, if confirmed, can be the evidence of new physics processes contributing to the $g-2$ value. The new experiment at Fermilab (E989) is now running to achieve 21 times the statistics of the BNL experiment and to reduce the uncertainty by a factor 4 (0.14 ppm).

1˙1. *The measurement.* – The a_μ measurement is based on the extraction of the anomalous precession frequency of the muon's spin in a magnetic field. We can define the anomalous precession frequency (ω_a) as the difference between the spin precession frequency and the cyclotron frequency. For relativistic muons, assuming that the magnetic field is uniform and the betatron oscillations of the beam are negligible, the $\overrightarrow{\omega}_a$ can be written as

$$\overrightarrow{\omega}_a = \overrightarrow{\omega}_s - \overrightarrow{\omega}_c = -\frac{q}{m}\left[a_\mu \overrightarrow{B} - \left(a_\mu - \frac{1}{\gamma^2-1}\right)\frac{\overrightarrow{\beta}\times\overrightarrow{E}}{c}\right], \tag{5}$$

where β is the particle speed in units of c, and the term $\overrightarrow{\beta}\times\overrightarrow{E}$ represents the contribution of the electric field. For the specific value of $\gamma = 29.3$ (*i.e.*, $p_\mu = 3.094\,\text{GeV}$) called *magic momentum*, the electric field term in eq. (5) vanishes, leaving just the B field term. Precision measure of $\overrightarrow{\omega}_a$ and of the magnetic field leads then to a measure of a_μ.

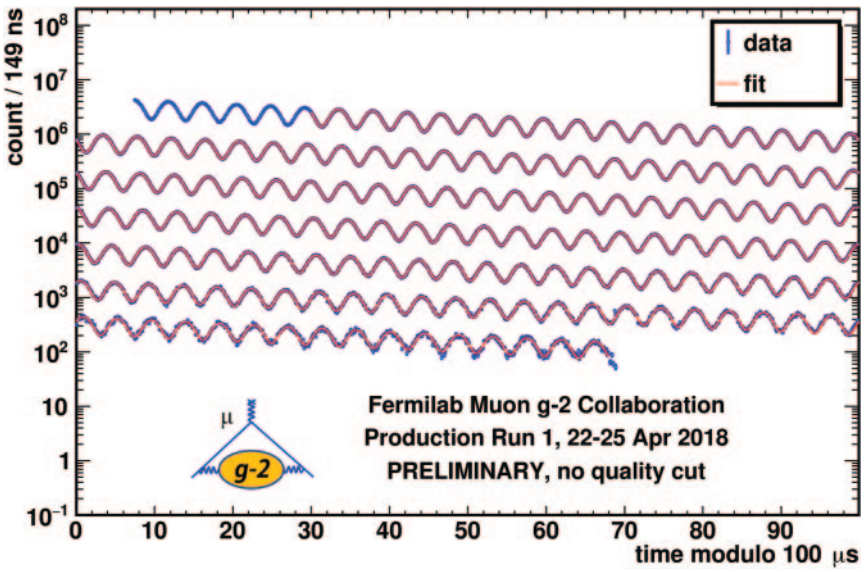

Fig. 2. – Preliminary Wiggle plot of the Muon $g-2$ experiment (E989) using ∼60 hour data. The curve is fitted with eq. (6).

Due to the parity violating decay of muons, there is a strong correlation between the high energy positrons' momentum direction and the muon's spin; counting the number of high energy positrons along the muon momentum axis as a function of time gives a curve that is the decay exponential modulated by the ω_a anomalous precession frequency, producing the so-called "Wiggle Plot" (fig. 2). The equation used for the fit, including corrections due to the beam dynamics ($C(t)$ for radial CBO and $V(t)$ for the vertical waist) and muon loss ($\Lambda(t)$) is

$$N(t) = N_0 e^{-\frac{t}{\tau}}[1 - A\cos(\omega_a t + \phi)] \cdot C(t) \cdot V(t) \cdot \Lambda(t) \tag{6}$$

2. – E989 experiment at FNAL

The Muon $g-2$ experiment at Fermilab aims to measure the muon's anomalous magnetic moment with a precision of 0.14 ppm, a factor 4 better than the BNL's E821 experiment. With this precision, the results can hopefully clarify the difference found at BNL.

The main part of the experiment is a 14 m superconducting storage ring producing a 1.45 T uniform magnetic field (shown in fig. 3) also used by the E821 experiment. A beam of positive muons produced by FNAL's accelerators chain is injected in the ring. Three fast kicker magnets put the injected muons in the magic orbit. Electrostatic quadrupoles provide vertical focussing of the beam. The field is measured by fixed NMR probes placed around the ring under and over the vacuum chamber. Regularly trolley runs are performed: a cylinder equipped with 17 NMR probes is placed inside the vacuum chamber and moved along all the ring to measure the field magnitude inside the storage region.

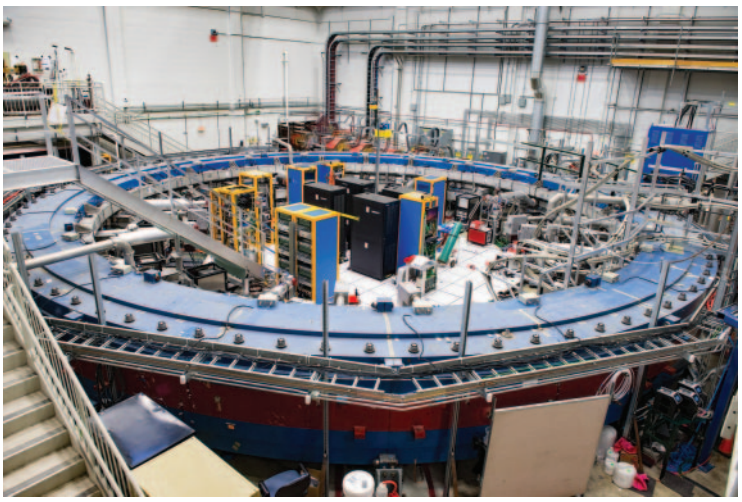

Fig. 3. – *One Ring to rule them all, One Ring to find them, One Ring to bring them all, and in the Darkness blind them.* (J. R. R. Tolkien, The Lord of the Rings).

2˙1. *The calorimeter system.* – The calorimeter system on the Muon $g-2$ experiment is, after the ring itself, the main part of the detector. The aim of the calorimeters is to precisely measure the arrival time and the energy of the decay positrons curling into the ring due to the magnetic field (fig. 4). There are in total 24 calorimeters outside the vacuum chamber along the inner circumference of the ring. Each calorimeter is placed right behind a radial window that allows positrons to exit the vacuum chamber minimizing the path in air.

A single calorimeter is composed of 54 Lead Fluoride Čerenkov crystals arranged in a 9×6 matrix. The material of choice is lead fluoride due to its characteristics: high density ($7.77\,\mathrm{g/cm^3}$), low Molière radius (1.8 cm for the Čerenkov light only), low radiation length ($X_0 = 0.93\,\mathrm{cm}$) and low magnetic susceptibility. Each crystal has an area of $2.5 \times 2.5\,\mathrm{cm^2}$ and a length of 14 cm ($\sim 15 X_0$). Crystals are wrapped in black Tedlar absorbtive wrapping to transmit only the direct Čerenkov light. The calorimeter's

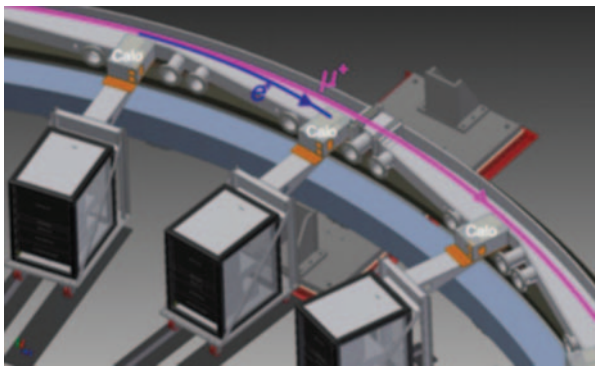

Fig. 4. – Drawing of the calorimeters position along the ring. The positrons have a smaller orbit due to the lower mass, so they curl inside the ring and are detected by the calorimeters.

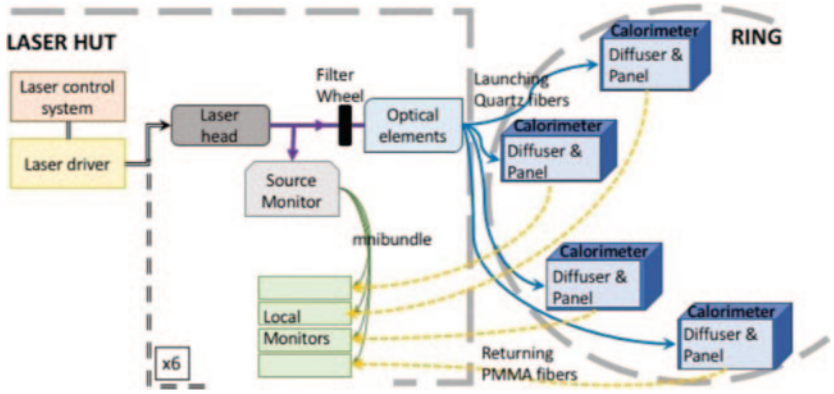

Fig. 5. – Sketch of the laser calibration system.

segmentation gives a better spatial resolution. This allows to better discriminate particles and therefore to reduce the pile up systematics. Moreover a Čerenkov crystal is faster than a scintillating one, so the time response of this calorimeter is smaller than the ones used for the E821 experiment. Faster crystals provide a better time resolution to discriminate pile up events and further reduce the systematics related. The light from each crystal is read by a Large Area Silicon Photomultiplier (SiPM) working in the Geiger mode. Each SiPM has an active area of $1.2 \times 1.2\,\mathrm{cm}^2$ with $50\,\mu$m pixels, that is well-matched with the crystal area [4].

On the down side, SiPMs are sensitive to temperature and bias voltage variations, so a high precision laser system, shown in fig. 5, was built and is operated by INFN to provide the SiPMs' gain calibration, keeping the systematic contribution to the measure at the level of 20 ppb.

There are 6 laser heads, each connected to 4 calorimeters via optical fibers cables. Each laser fires a light pulse with the same wavelength of the Čerenkov radiation emitted by the crystals (405 nm) and the light is evenly distributed to all the crystals. Before the muon injection (fill), typically once every 10 muon fills, a laser pulse is sent to the calorimeters and their response is measured to keep track of the gain and eventually correct for any variation. The signal also provides a time synchronization of the calorimeters.

Any variation in the laser intensity is checked with a Source Monitor (SM) and a Local Monitor (LM). The source monitor uses two PIN diodes to measure the laser intensity and to check for any variation. A third light detector is an 8 mm diameter photomultiplier to double check the diodes stability, and whose stability is checked with a low counts ^{241}Am source. The Local Monitor instead is the system that checks for variations in the light distribution system. A return optical fiber brings the light from the diffusion panel of the calorimeter again into the laser hut. The return light intensity is measured with a traditional photomultiplier and is compared to the laser light from the source monitor. In this way it is possible to keep under control any variation both in the laser itself or in the distribution fibers. The laser system is measured to be stable at the per-mil level in the time period of the measure ($700\,\mu$s). See refs. [5, 6] and references therein for details.

2˙2. *The tracker.* – The tracker detector measures the beam profile and its position, without affecting the beam itself. The system has two stations, one at $\sim$180° and one at $\sim$270° along the ring placed before calorimeters number 13 and 19 (fig. 6). Each station

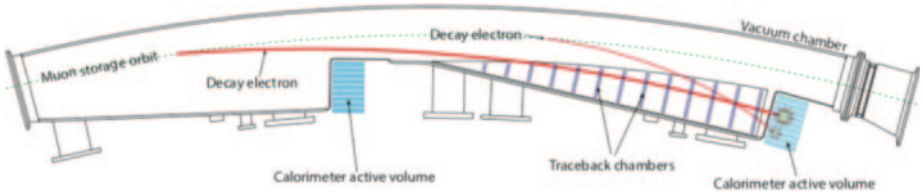

Fig. 6. – Tracker (1 station) scheme. The beam goes from left to right.

is made by 32 planes of drift tubes arranged in 8 modules, each module has 4 straw planes. The straws are arranged in a stereo pattern, with an angle of $\pm 7.5°$ from the vertical direction. This arrangement provides both the x and y position of the track. The tubes are filled with a $50:50$ mixture of argon and ethane.

When a muon decays near the tracker stations, the tracker measures in each plane the positron's x and y coordinates. The trajectory is reconstructed fitting the points from each straw plane. From the trajectory, going backward inside the ring, the decay vertex is also reconstructed. Knowing the position of the decay vertex is possible to measure the xy beam distribution without affecting the beam itself, so the straw tracker provides a beam measure during the whole data taking.

From the track curvature and from the field intensity, it is possible to measure the particle's momentum. It is also possible to match the particles crossing the tracker and the calorimeter in a time window of few nanoseconds, this process is called "Calo-Track Matching". In this way it is possible to identify a particle by the energy-momentum relation and therefore identify lost muons.

3. – Energy calibration

Using a known energy process it is possible to determine the conversion factor between the charge in the SiPM and the energy deposited from the incident particle. This procedure, which goes under the name of energy calibration, can be obtained in two different ways: the endpoint of the positron spectrum and the energy peak produced by minimum ionizing particles (MIP) in the calorimeter.

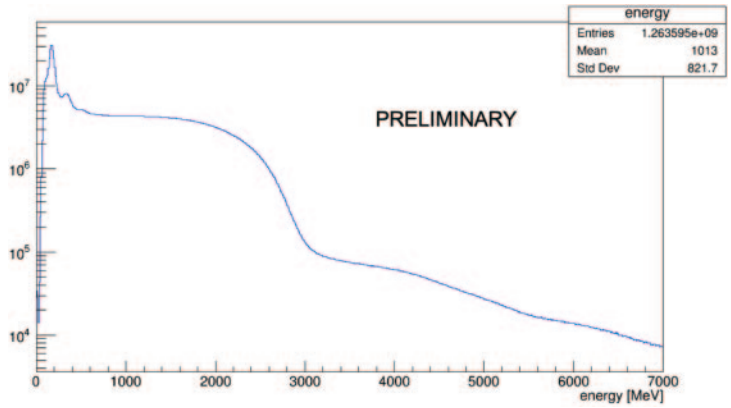

Fig. 7. – Energy spectrum as measured by the calorimeters. It is possible to see the long tail caused by pile up events.

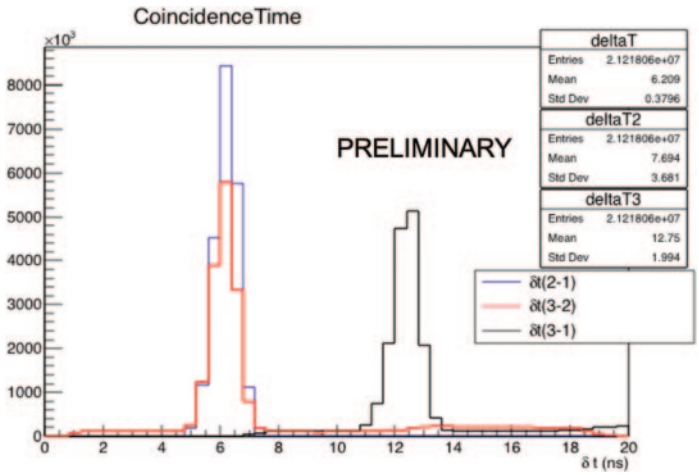

Fig. 8. – $\delta t = t_i - t_j$ distribution for triple coincidence events. A Gaussian fit is applied just to identify the mean value of the peak.

3˙1. *Endpoint*. – The endpoint of the energy spectrum is fixed by the kinematics of the experiment. The momentum of the μ^+ entering the storage ring is selected at 3.094 GeV, the energy is $E_\mu = 3.102$ GeV. This energy puts an upper limit to the energy of a decay positron. However, due to the pile up events, the spectrum does not end precisely at 3.1 GeV but shows a long tail (fig. 7).

3˙2. *MIP peak*. – The MIP peak is visible in fig. 7 at low energies, and is caused by muons that exit the vacuum chamber and hit two or more calorimeters. These muons deposit a reasonably fixed amount of energy in a 14 cm crystal. This deposit can be predicted with a Monte Carlo simulation of the particle traversing the calorimeter and

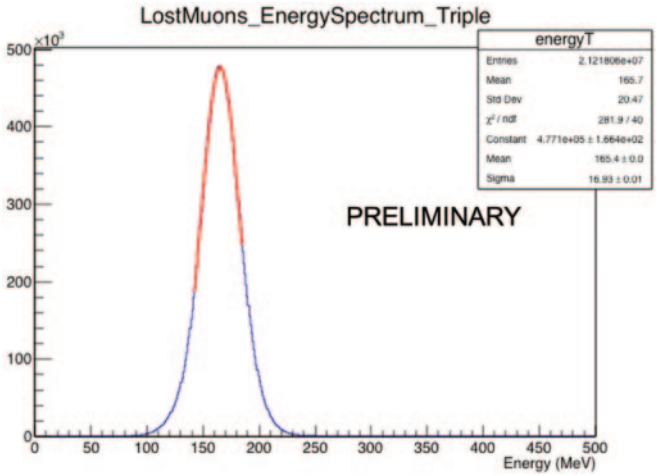

Fig. 9. – Energy spectrum for lost muons. As expected by the Bethe-Bloch formula, 3.1 GeV muons in PbF_2 crystals deposit ∼166 MeV. The peak can be used to calibrate the crystals.

confronted with the charge measured by SiPMs. One way to identify lost muons is to check for a signal in coincidence in two or three consecutive calorimeters. The requests to flag an event as a muon are:

- timing: $\delta t = t_i - t_j \leq (i-j) \cdot 1.25\,\text{ns}$, where i and j are the calorimeters number in a coincidence;
- energy: $140 \leq E \leq 220\,\text{MeV}$;
- hit localized only in one crystal (ionization due to muons is very localized).

In fig. 8, the distribution of the variable $\delta t = t_i - t_j$ for all the calorimeters is shown. The plot shows the peak at $\sim$6.2 ns for two consecutive calorimeters and $\sim$12.4 ns for the two non consecutive ones as expected (since the distance between calorimeters is about 1.8 m). The energy spectrum (fig. 9) shows a peak around 165 MeV, compatible with what was expected from the Bethe Bloch energy loss. This peak, together with a Monte Carlo simulation of lost muons, can be used for the energy calibration of the crystals.

3˙3. *Conclusions*. – The new Muon $g-2$ E989 experiment at Fermilab will provide the measurement of the muon's anomalous magnetic moment with a precision of 0.14 ppm. A precise measurement of the anomalous precession frequency together with a high precision magnetic field measurement will lead to this goal. During Run 1 (2018), the experiment collected almost twice the positrons collected at the BNL experiment. A first result with almost the same statistical power as the BNL result is expected before summer 2020.

* * *

This work was supported by the Department of Energy offices of HEP and NP (USA), the National Science Foundation (USA), the Istituto Nazionale di Fisica Nucleare (Italy), the Science and Technology Facilities Council (UK), the Royal Society (UK), the European Union's Horizon 2020 research and innovation programme under the Marie Skłodowska-Curie grant agreements No. 690835 (MUSE), No. 734303 (NEWS), MOST and NSFC (China), MSIP and NRF (Republic of Korea).

REFERENCES

[1] Particle Data Group (Tanabashi M. *et al.*), *Phys. Rev. D*, **98** (2018) 030001.
[2] Muon $g-2$ Collaboration (Bennet G. W. *et al.*), *Phys. Rev. D*, **73** (2006) 072003.
[3] Keshavarzi A. *et al.*, *Phys. Rev. D*, **97** (2018) 114025.
[4] E989 collaboration, *Muon $g-2$ Technical Design Report*.
[5] Driutti A. *et al.*, *Nucl. Instrum. Methods Phys. Res. A*, **936** (2019) 98.
[6] Anastasi A. *et al.*, *The laser calibration system of the Muon $g-2$ experiment at Fermilab*, arXiv:1906.08432 [physics.ins-det].